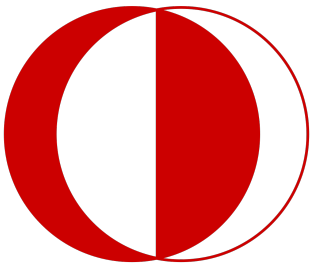

Middle East Technical University

EE430 Digital Signal Processing - Project 2

Range and Speed Estimation by Short Time Fourier Transform

Group 6

Okyanus Oral - 2305134

Sezan Mert - 2232445

Table of Contents

Chapter 1

Introduction

Velocity or range estimations of vehicles by using active sensors such as radars or sonars or by using passive sensors are problems that are studied intensively. Doppler-based motion estimation is one of the suggested solution methods to this problem [1].

In this project, the speed and the range of the vehicle is aimed to be estimated by considering the Doppler effect on the observed signals. The signal emitted by the vehicle was modelled as sinusoidal pulse and rectangular windowed linear chirp signals with additive Gaussian white noise. Then by using the spectrogram of the observed signals as observed by a stationary observer, the range and the velocity of the vehicle was estimated. In order to evaluate the performance of the algorithms, Monte Carlo simulations were conducted. From Monte Carlo trials, the mean absolute percentage error (MAPE) of the speed and distance estimations and standard deviation of this error are found. The effects of signal-to-noise-ratio (SNR), short time fourier transform (STFT) window length, STFT window overlap, initial frequency of emitted signals, velocity of the emitter, bandwidth (for linear sinusoidal chirp) on the written estimation algorithm were tested. The results are examined with Self Organising Maps and discussed.

The following chapters include theoretical background and suggested methods for the solution of the problem. The implemented solution algorithms are explained and the results are shown. The effects of aforementioned parameters are observed and the causal factors for the observed performance results are explained. Finally learning outcomes and gained experiences are mentioned in the conclusion.

Chapter 2

Theoretical Background

In the scenario given for this project, the vehicle moves towards a stationary observer with a constant speed while emitting a short pulse of signal. The emitted signal, either a sinusoidal pulse or a rectangular windowed linear chirp, moves with a constant speed of c = 340 m/s and the starting time of the signal is known.

If we are to model the signals emitted by this moving source as

$$s_1(t) = A\sin(\Omega_0 t)(u(t) - u(t-\Delta))$$

and

$$s_2(t) = \begin{cases} A\cos\left(2\pi(f_0 t + \frac{m}{2\Delta}t^2)\right) & 0 \leq t \leq \Delta \\ 0 & otherwise \end{cases}$$

then the observed signals can be expressed as

$$\widehat{s_1}(t) = s_1\left(\left(\frac{c}{c \pm v}\right)(t - t_0)\right)$$

and

$$\widehat{s_2}(t) = s_2\left(\left(\frac{c}{c \pm v}\right)(t - t_0)\right)$$

In other words, the observed signals will be warped due to the Doppler effect with the coefficient $\frac{c}{c \pm v}$ (minus for approaching source and plus for departing source) and the signal will reach the observer in a delayed manner due to the distance between the source and the observer. Therefore, the duration of the observed signal will change.

2.1 Velocity and Distance Estimation by Using STFT

Frequency shift of the emitted signal from approaching and departing vehicle is used to infer the speed of the vehicle. From the boundary of frequency shifts, arrival time is estimated. Both arrival time and speed estimates are used to find the initial distance of the vehicle.

The frequency of the approaching signal $f_a(t)$ and the departing signal $f_d(t)$ is Doppler shifted from the original frequency emitted $f_o(t)$.

$$f_a(t) = f_o(t)\frac{c}{c-v}$$

$$f_d(t) = f_o(t)\frac{c}{c+v}$$

If approaching and departing frequencies can be detected correctly the speed v of the vehicle can be found from the ratios obtained from these frequencies.

For an emitted sinusoidal wave of constant frequency, direct substitution of the measured frequencies can be used to find the speed of the vehicle.

$$v = c \cdot \frac{f_a - f_d}{f_a + f_d}$$

For an emitted sinusoidal linear chirp wave, direct substitution of the slopes of the frequency can be used to find the speed of the vehicle.

$$v = c \cdot \frac{\dot{f}_a(t) - \dot{f}_d(t)}{\dot{f}_a(t) + \dot{f}_d(t)}$$

The arrival time t_a of the vehicle is the time instance which the observed frequency transits from $f_a(t)$ to $f_d(t)$ and is discontinuous for an observer located on the pathway.

$$\Delta x = v \cdot t_a$$

2.2 Determination of Ranges of the Parameters

The parameters Δ, f_o, m, t_0 and v are determined by considering the other parameters such as F_s, also by making assumptions and restricting the system with reasonable conditions.

2.2.1 Sampling Frequency: $F_s = 44.1kHz$

The propagation rate of the signal is given as 340 m/s which is approximately equal to the speed of sound (343 m/s). Hence the emitted signal is assumed to be a sound signal. To set an upper bound on sampling it was further assumed that frequency of this signal will not reach the ultrasound and stay in the audible frequency range for

humans. Therefore, as a standard for audio signal processing, the sampling rate, F_s, is chosen as 44.1 kHz.

2.2.2 Speed: $v \epsilon\{16.67m/s, 257.22m/s\}$

While experimenting with parameters, it was observed that errors of the estimations peak on slower vehicles (since for slower vehicles $f_a(t_a) \approx f_d(t_a)$ and with negligible difference on frequency, accuracy of estimations decrease). To limit the number of parameters on grid search to a reasonable minimum, observable minimum and maximum speeds of vehicles are selected. With the selected minimum value, an increase; with the selected maximum value, a decrease on estimation errors were intended to be observed and logged on tests. The observable minimum speed v_{min} is selected as the average speed of a car on a city road, around 60 km/h or equivalently 16.67 m/s .The observable maximum speed v_{max} is selected as the speed of a commercial airplane, around 575 mph or equivalently 257.22 m/s .

2.2.3 Initial Frequency: $f_o \epsilon\{100Hz, 4kHz\}$

Considering Doppler shift and the bandwidth of the chirp signal, maximum initial frequency is decided to be set below $F_s/2$. To give a meaningful upper bound for the initial frequency, in accordance with the real-life vehicles, maximum initial frequency is set to a high frequency engine noise of 4kHz (which is representative of both aircraft and automobiles) [2] [3].

A similar discussion with the selection of speed is also present on the selection of the lower bound for the initial frequency. As the initial frequency decreases, even if the Doppler shift is high, $f_a(t_a)$ approaches to $f_d(t_a)$. As $f_a(t_a)$ and $f_d(t_a)$ gets closer, the separation of frequencies at arrival instant, t_a, becomes harder to detect due to limited frequency resolution from STFT window lengths. Hence the accuracy of estimations decrease. For the low end of initial frequencies, a considerably low engine noise of 100 Hz [2] [3] is set. Accuracy decrease on low initial frequency and accuracy increase on high initial frequency is intended to be observed and logged on tests.

2.2.4 Duration:Δ=2 seconds (Approach: 1 s, Depart: 1 s)

The vehicle is conditioned to emit signals at least one second before it reaches the observer and also it must continue to emit for at least one more second after it passes the observer.

With varying values for the speed, observed signal duration varies both for approach and departing cases. The observed duration is related with the duration of the signal with the expression $\widetilde{\Delta} = \Delta - t_0$. The delay, t_0, depends only on the speed for $\Delta = 1$ second which will be explained below more in detail. The higher the speed, higher the delay and therefore higher the shrink in the observed duration (for the approach).

On estimations of speed and distance, for constant frequency sinusoidal and for the sinusoidal linear chirp, the algorithms are prone to the insufficient duration of observations. Hence by selecting constant duration for the emitted signal, the effect of speed on the observed duration, thus the effect on accuracy of estimations is planned to be observed.

2.2.5 Delay: $\mathbf{t_0}$ $\epsilon\{0.049s, 0.76s\}$

The delay parameter is directly related with the range of the vehicle. If the initial distance of the vehicle to the observer is x_0, the delay that the observer perceives is $t_0 = \frac{x_0}{c}$. Since the vehicle is conditioned to start emitting signals one second before reaching the observer, the delay becomes dependent only to the speed of the vehicle. Hence, the relation turns into $t_0 = \frac{v \cdot 1}{c}$ seconds. The speed values are chosen as 16.67m/s and 257.22 m/s. According to the relation, the t_0 values will take values 0.049 seconds and 0.76 seconds, respectively. Since the delay occurs in the code depending on the value of the speed, the parameter variation was not explicitly shown as a grid parameter in the results.

2.2.6 Bandwidth: $\mathbf{m}$ $\epsilon\{200Hz, 1300Hz\}$

Upper bound for bandwidth without any aliasing is found from the fixed parameters. The maximum upper bound is calculated to be $m_{max} = (F_s \frac{(c - v_{max})}{2c} - f_{o,max}) = 1368.39Hz$. Maximum bandwidth is

set to 1300 Hz by setting a margin for additional measure. In terms of observing the trend of performance at high frequencies, the set value 1300 Hz does not impose any deviation when compared with 1368.39 Hz.

Similar to discussions of lower limits on selection of speed and initial frequency, with lower bandwidths $\dot{f}_a(t) \approx \dot{f}_d(t)$ the slopes do not deviate significantly, hence the accuracy of estimations decrease.

For a meaningful comparison with lower initial frequency, 100 Hz, minimum bandwidth is selected as 200Hz. This bandwidth yields 100Hz/s frequency slope with the specified total duration of 2 seconds.

Chapter 3

Implemented Algorithms for Estimations

In order to perform the computation steps (see Section 2.1) for the estimations of speed and distance, dominant frequency of the observed signal with respect to time is found with STFT based method. Then relevant algorithms to estimate f_a,f_d for sinusoidal waves of constant frequency and $\dot{f}_a(t)$,$\dot{f}_d(t)$ for sinusoidal linear chirp waves are applied.

3.1 Estimation of Dominant Frequency with STFT

1. With the specified parameters for STFT, spectrogram of the signal is obtained (see Fig. 3.1).

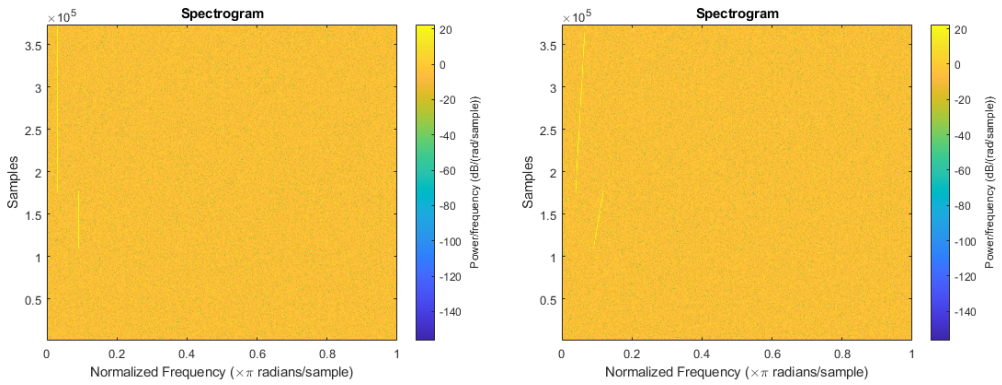

(a) Sinusoidal Waves of Constant Frequency.

(b) Sinusoidal Linear Chirp.

Figure 3.1: Spectrogram of signals with parameters: Fs=44100 Hz, f_o =1000 Hz, SNR=-1 dB, speed=170, frequency slope= 200 $\frac{Hz}{s}$, window length = 2500 samples, overlap pervcent = 90% .

2. The signals contain additive Gaussian white noise with zero mean. Hence there is an offset power on the spectrogram. If the offset is negligibly small (corresponds to lower SNR values) the frequencies corresponding to sinusoids can be seperated from that of noise. By thresholding with respect to the power peaks of the spectrogram, a mask of sinusoidal frequencies is obtained (see Fig. 3.2).

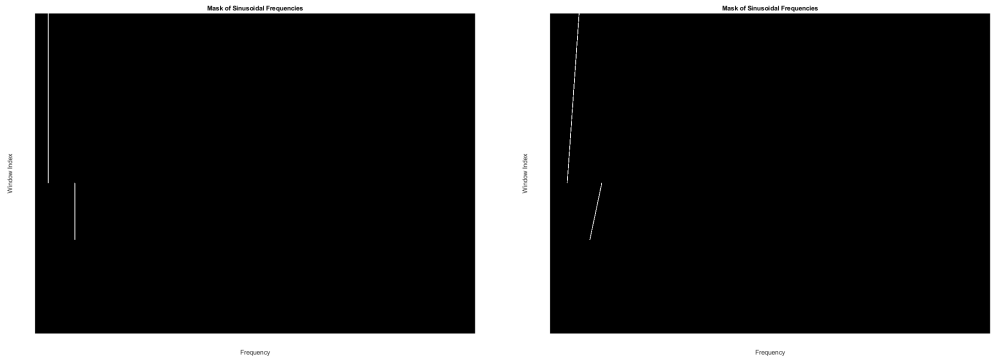

(a) Sinusoidal Waves of Constant Frequency. (b) Sinusoidal Linear Chirp.

Figure 3.2: Sinusoidal Frequency Mask of signals with parameters: Fs=44100 Hz, f_o =1000 Hz, SNR=-1 dB, speed=170, frequency slope= 200 $\frac{Hz}{s}$, window length = 2500 samples, overlap pervcent = 90% .

3. The frequency mask contains *logical 1*'s at the corresponding frequency bins and *logical 0's* otherwise. Multiplying each bin with the respective frequency value yields an image of frequency stripes. By averaging this image of frequency stripes on each time bin, *dominant frequency graph* with respect to time is obtained (see Fig. 3.3).

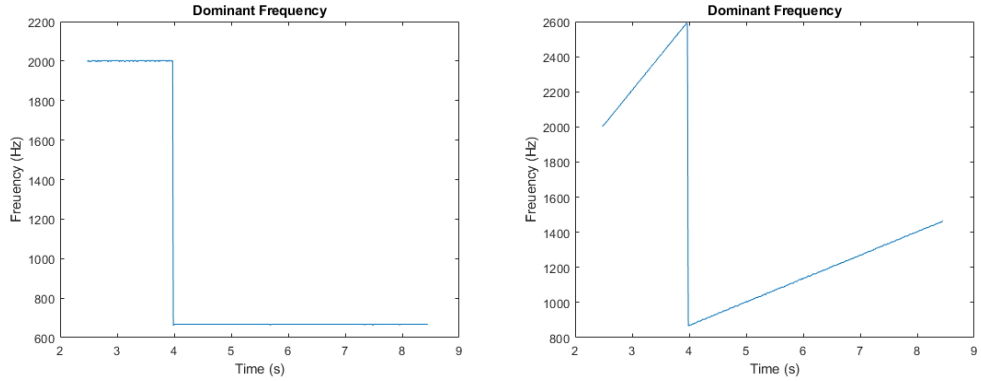

(a) Sinusoidal Waves of Constant Frequency. (b) Sinusoidal Linear Chirp.

Figure 3.3: Dominant Frequency Graph of signals with parameters: Fs=44100 Hz, f_o =1000 Hz, SNR=-1 dB, speed=170 m/s, frequency slope= 200 $\frac{Hz}{s}$, window length = 2500 samples, overlap pervcent = 90% .

3.2 Estimation of f_a,f_d,t_a for Sinusoidal Waves of Constant Frequency

1. From the maximum and minimum frequencies on dominant frequency graph, a threshold value to separate approaching and departing frequencies is obtained. The dominant frequency graph is separated to its high and low frequency components. The corresponding time instance for this separation is arrival time t_a.
2. The frequency average of high frequency components corresponds to approaching frequency f_a and the frequency average of low frequency components corresponds to departing frequency f_d.
3. Using f_a,f_d and t_a, speed and initial distance of the vehicle is estimated (see Section 2.1).

3.3 Estimation of $\dot{f}_a(t)$,$\dot{f}_d(t)$ and t_a for Sinusoidal Linear Chirp

1. Dominant frequency graph is two piece-wise linear functions. With forward iteration on time samples, using least squares estimate on the samples read, a line is fitted to the dominant frequency data. At each step in forward iteration, error of the new data point to its estimate is logged. The logged error peaks on the discontinuity at arrival time t_a (see Fig. 3.4, the index of maximum error matches with the index of t_a).
2. With t_a found, two lines that corresponding to $f_a(t)$ and $f_d(t)$ are fitted. The frequency slopes $\dot{f}_a(t)$,$\dot{f}_d(t)$ of the approaching and departing vehicle are calculated.
3. Using$\dot{f}_a(t)$,$\dot{f}_d(t)$ and t_a, speed and initial distance of the vehicle is estimated (see Section 2.1).

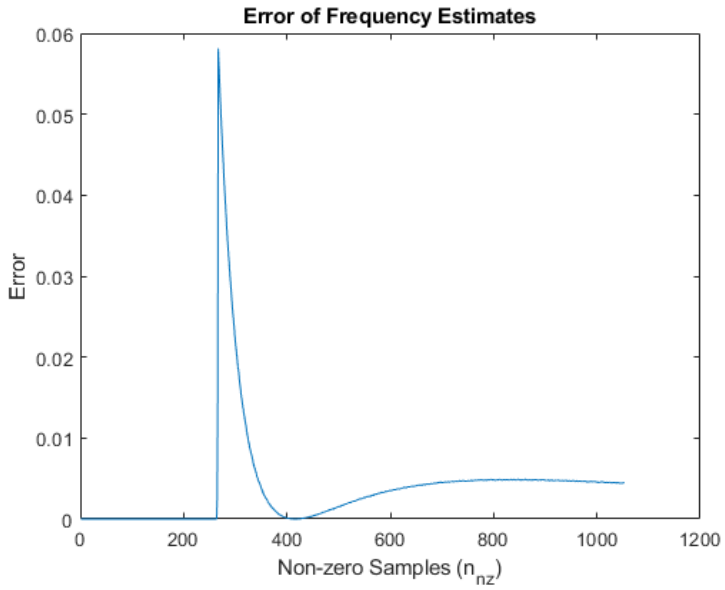

Figure 3.4: Piece-wise linear frequency estimation error of chirp signal with parameters: Fs=44100 Hz, f_o =1000 Hz, SNR=-1 dB, speed=170, frequency slope= 200 $\frac{Hz}{s}$, window length = 2500 samples, overlap pervcent = 90% .

Chapter 4

Tests of Estimations

4.1 Test Objectives and Parameters

Trends of estimation (vehicle speed and initial distance) performance on different SNRs, STFT window lengths and overlap percentages are tried to be observed. For each SNR, window length, overlap percentage triplet; the grid parameters, speed of the vehicle, initial frequency and bandwidth, are varied. At each variation 30 Monte Carlo trials by updating the superposed noise, are made. The number of trials are chosen as 30 according to the minimum sufficient trial size for one dimension of freedom stated in Central Limit Theorem [4].

SNR ϵ $\{-2dB, -1dB, 0dB, 1dB\}$. With higher SNR it is expected to observe less error on estimates.

STFT window length ϵ $\{1000samples, 2000samples, 5000samples,$ $8976samples\}$. The window size effects both the time and frequency resolution. To observe the frequency split at t_a, the sample length of the window should be selected to yield a frequency resolution capable of showing the minimum frequency difference due to Doppler shifts. The minimum frequency difference δf_{min} at t_a is obtained with the relation $\delta f_{min} = 2 f_{o,min} \frac{c.v_{min}}{c^2 - v_{min}^2}$ where v_{min} is the minimum speed and $f_{o,min}$ is the minimum initial frequency. If the main lobe width of the Hamming window (used window type due to -40 dB side lobe attenuation [5]) is equated to δf_{min} then the the required sample size is obtained to be 8976. Hence the upper window length limit, maximum required frequency resolution, is set. To observe the effects of lesser frequency resolution on estimation performance; tests are also conducted with windows of 1000, 2000 and 5000 samples. Especially on low initial frequencies, low bandwidths and low speeds, with increasing frequency resolution, accuracy increases.

STFT window overlap ϵ $\{50\%, 75\%, 90\%\}$. With higher overlap percentages especially on high window sizes it is expected to observe less

error on estimates.

The speed and range estimations obtained after N=30 Monte Carlo trials are used to calculate the Mean Absolute Percentage Error (MAPE) and the error standard deviation with the following equations:

$$MAPE = \frac{1}{N} \sum_{i=1}^{N} \frac{|est_i - act_i|}{act_i}$$

$$ErrorSTD = \sqrt{\frac{\sum_{i=1}^{N} (err_i - \mu_{err})^2}{N}}$$

where,

$$est_i\text{: i}^{\text{th}}\text{ estimation}$$
$$act_i\text{: i}^{\text{th}}\text{ data}$$
$$err_i \stackrel{\Delta}{=} est_i - act_i$$
$$\mu_{err} \stackrel{\Delta}{=} \frac{1}{N} \sum_{i=1}^{N} err_i$$

The obtained multi-parameter results are presented with Self Organizing Maps (SOM). SOM is a type of neural network model that enables visualisation of dependencies on multidimensional data as a two dimensional image. The maps are obtained with the used Self Organising Map application as in [6].

Self Organising Maps create a 2D plot for each parameter separately. The colors of these plots represent the values of these parameters. The coordinates are same for all plots, hence for all parameters. Therefore, from the maps, one can observe the dependencies of different parameters with respect to each other. For instance, in Figure 4.2 (a) the frequency plot takes the value 200 Hz for coordinates {A:D, 3:5}, shown in blue. In all the other maps, the coordinates {A:D, 3:5} also correspond where the frequency is equal to 200 Hz. In the Figure 4.2 (f), one can see that the coordinates of the highest error match with 200 Hz initial frequency and speed of 16.67 m/s. The legends for the values of the colors are given under each map and the minimum and maximum values are written on the black strip under the legend.

4.2 Test Results of Sinusoidal Pulse as Emitted Signal

Since the error deviates between 10^{-5} and 1, the base 10 logarithm of the MAPE is taken in order to have a better understanding of the error distribution.

4.2.1 Speed Estimation

The Figure 4.1 (f) shows the values of $log_{10}(MAPE)$ for speed estimation relative to other parameters that are f_0, window overlap, window length, SNR and speed. From Figure 4.1 the followings are observed;

- The highest logarithmic MAPE value is at {A:B, 1}. Corresponding,
  - *Initial Frequency = 200 Hz (Low)*
  - Overlap Percentage = All values present.
  - *Window Length = 1000,2000 samples(Low, Moderately Low)*
  - SNR : All values present.
  - *Speed = 16.67 m/s (Low)*

* The low frequency and low speed values results in a subtle change in the frequency at t_a. Also as the window length decreases, the frequency resolution decreases. Hence, estimation of speed becomes inaccurate, causing the observed logarithmic MAPE values at their highest.

* Especially in the A1 cell, the effect of change of SNR values on the MAPE error is significant. SNR value increases from the upper left corner of the cell through the lower right corner of the cell. Simultaneously, the MAPE error increases in the same direction.

* The overlap percentage does not seem to be correlated with the MAPE error observations.

- Lowest logarithmic MAPE error values are observed at {D, 4}.Corresponding,
  - *Initial Frequency = 4000 Hz (High)*
  - *Overlap Percentage = 50%, 75% (Low, Moderate)*

  - *Window Length = 5000, 8976 samples (Moderately High, High)*
  - SNR : All values except the highest is present.
  - *Speed = 257.22 m/s (High)*

* The high speed and frequency values enable distinguishing two different frequencies. Also the high window length increases the frequency resolution of the spectrogram. As a result, the lowest MAPE is observed.

* The relatively low SNR values has also seemed to have effect on this low error.

- Another high logarithmic MAPE value is at {D, 1}. Corresponding,
  - *Initial Frequency = 4000 Hz (High)*
  - *Overlap Percentage = 75%, 90% (Varying)*
  - *Window Length = 1000 samples (Low)*
  - *SNR : -2 dB (Low)*
  - *Speed = 16.67 m/s (Low)*

* Even though the initial frequency is high; low speed, low SNR value and low number window samples result in high percentage error since all of these factors distort frequecy accuracy.

* Window overlap is observed not to have a significant effect on the MAPE.

- Sligh MAPE increase in {A:B,4:5}. Corresponding,
  - Initial Frequency = 200 Hz (Low)
  - Overlap Percentage = All values present.
  - *Window Length = All values present*
  - *SNR : 1 dB (High)*
  - *Speed = 257.22 m/s (High)*

* When the MAPE at {A:B,5} is compared with the MAPE at {A:B,4}, it can be observed that with decreasing window length

error increases. This was expected and supports the inferred results form {A:B,4:5}. With lower length of windows, frequency resolution decreases. The estimation of speed is directly prone to frequency resolution since the calculations utilise the estimated approach and depart frequencies.

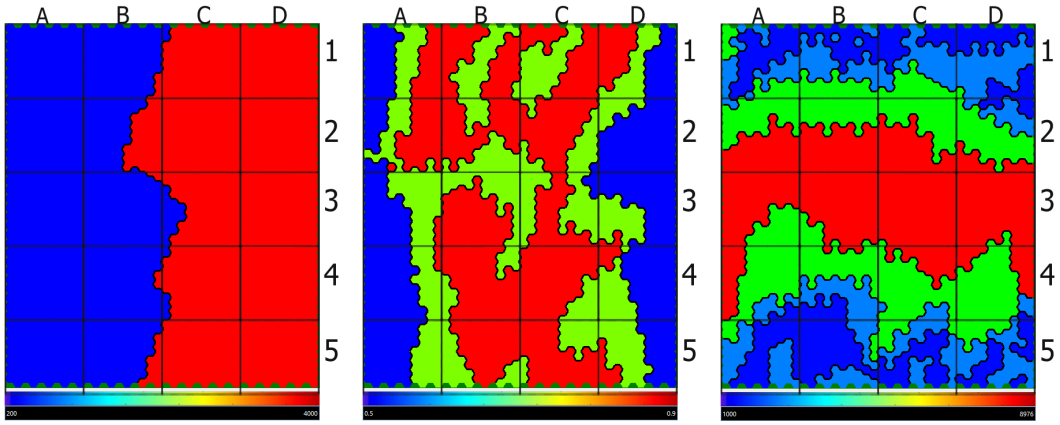

(a) Frequency Values of the Signal.

(b) Overlap Values for the STFT.

(c) Window Length Values for the STFT.

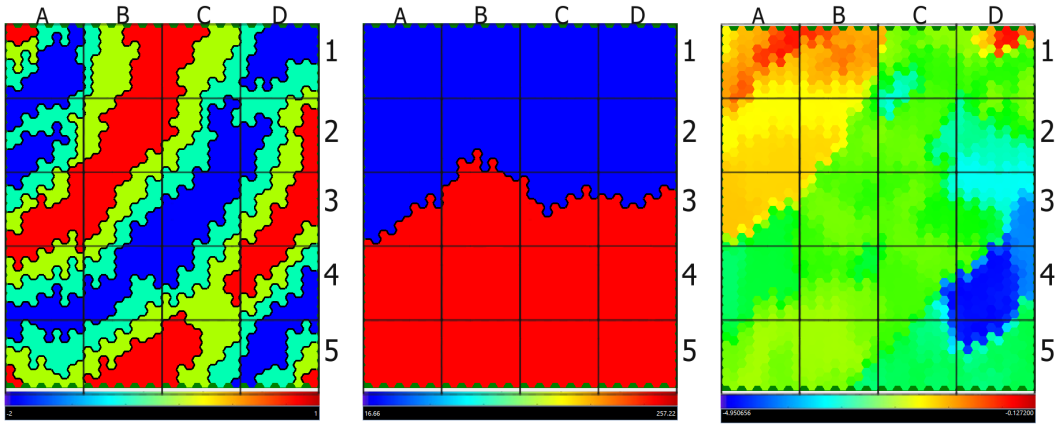

(d) SNR Values for the Additive Gaussian White Noise.

(e) The Speed of the Vehicle.

(f) Logarithmic Error Distribution

Figure 4.1: Self Organizing Maps of the Parameters for Speed Estimation with the Sinusoidal Pulse.

4.2.2 Distance Estimation

The Figure 4.2 (f) shows the values of $log_{10}(MAPE)$ for distance estimation relative to other parameters that are f_0, window overlap,

window length, SNR and speed.

Remark: The distance is estimated by using the estimated speed as explained in Section 2.1. For this reason, parameter changes that cause errors in the speed estimation also effects the errors in distance estimation.

From Figure 4.2 the followings are observed;

- The highest logarithmic MAPE value is at {C:D, 5}. Corresponding,
  - *Initial Frequency = 200 Hz (Low)*
  - *Overlap Percentage = 75%, 90% (Varying)*
  - *Window Length = 1000 samples (Low)*
  - SNR : All values present.
  - *Speed = 16.67 m/s (Low)*

  * The low speed and low initial frequency, results in a more subtle frequency change at arrival time t_a. Hence, it is harder to detect this time instance under these conditions and a high error is observed.

  * The low window length increases the time resolution and eases the detection of t_a. On the other hand, it decreases the accuracy of frequency detection resulting in an inaccurate speed estimation. Since the distance is obtained by multiplication of speed and t_a, it can be concluded that the error in the speed dominates the error of distance estimation.

  * The effect of window overlap and SNR are thought to be not significant since their values vary during this high error occurrence.

- The lowest error value is observed in the coordinates {A:B, 1}. Corresponding,
  - *Initial Frequency = 4000 Hz (High)*
  - *Overlap Percentage = 90% (High)*
  - *Window Length = 1000 (Low)*
  - SNR : All values present.

  - *Speed = 16.67 m/s (Low)*

* High frequency and high speed yields a significant change of frequency at t_a. Also small window length enhances the time resolution with high overlap values. All of these factors result in accurately found distance values, thus, low error.

* Since the SNR values change during this low error occurrence, it is considered not to have a significant effect.

- The lowest error value is observed in the coordinates {C:D, 5}.
  - *Initial Frequency = 200 Hz (Low)*
  - *Overlap Percentage = 25% (Low)*
  - *Window Length = 5000 (Moderate)*
  - SNR : All values present.
  - *Speed = 16.67 m/s (Low)*

* Despite the low frequency and low speed, detection of t_a seemed not to be effected due to high SNR values.

* The window length is moderate and this enables the accurate speed estimation. The effect of relatively long window length is compensated by the window overlap, hence the time of arrival estimation is not distorted much. All in all, the low logarithmic MAPE values are observed in the given coordinates.

4.3 Test Results of Rectangular Windowed Linear Chirp as Emitted Signal

The test results for the rectangular linear chirp, unlike the test results for sinusoidal pulse, are plotted without computing the logarithm of the MAPE. The logarithm computation was unnecessary since the deviation of error for this case is only between 10^{-2} and 1.

4.3.1 Speed Estimation

The Figure 4.3 (g) shows the MAPE values for the distance estimation relative to the parameters f_0, window overlap, window length,

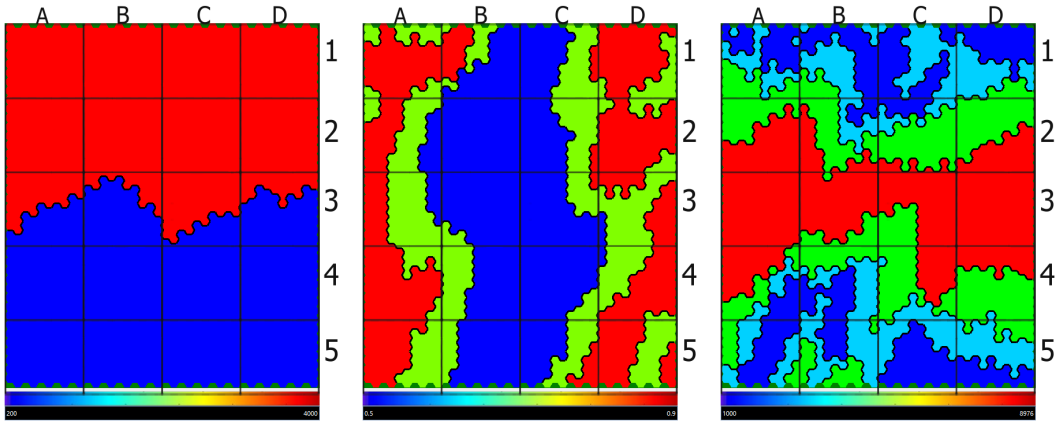

(a) Frequency Values of the Signal.

(b) Overlap Values for the STFT.

(c) Window Length Values for the STFT.

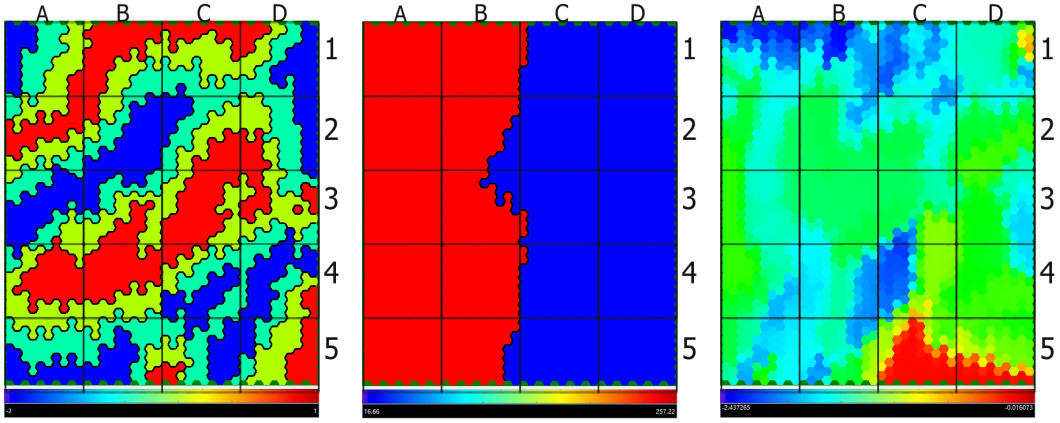

(d) SNR Values for the Additive Gaussian White Noise.

(e) The Speed of the Vehicle.

(f) Logarithmic MAPE Distribution

Figure 4.2: Self Organizing Maps of the Parameters for Distance Estimation with the Sinusoidal Pulse.

SNR, speed and bandwidth when the emitted signal is a rectangular windowed linear chirp. From the Figure 4.3 the followings are observed,

- The highest error value is observed in the coordinates {C, 2}. Corresponding,
  - *Initial Frequency = 4000 Hz (High)*
  - *Overlap Percentage = 90% (High)*
  - *Window Length = 8976 (High)*
  - SNR : All values present.

  - *Speed = 16.67 m/s (Low)*
  - *Bandwidth = 200 Hz (Low)*

* High frequency and high window length would effect the speed estimation in a positive way. However, the bandwidth parameter and speed is low which makes it harder to detect the change in the slope. Thus, the speed estimations become inaccurate.

* The effects of SNR and window overlap is seemed not to have any significant effect on the MAPE.

- A relatively high error value is observed in the coordinates {D, 3}. Corresponding,
  - *Initial Frequency = 200 Hz (Low)*
  - *Overlap Percentage = 50% (Low)*
  - *Window Length = 1000 (Low)*
  - *SNR = 0 dB(Moderately High)*
  - *Speed = 16.67 m/s (Low)*
  - *Bandwidth = 200 Hz (Low)*

* The parameters contribute to the high error with the decreasing frequency accuracy due to short window length and decreasing observability of frequency slopes due to low frequency, low speed and low bandwidth parameter.

* The relatively high SNR value is expected to lower the error, however, with all the other parameters contributing to worsen the error, the effect of SNR was not observable.

* The window overlap is seemed not to have any significant effect on the MAPE error.

- For the other values of the parameters, the algorithm is observed to have a moderate to high performance.

4.3.2 Distance Estimation

The MAPE values of the distance estimation varying with f_0, window overlap, window length, SNR, speed and bandwidth parameter m is presented in the Figure 4.4 (f).

Remark: The distance is estimated through the speed by using the relation explained in Section 2.1. Therefore, the parameter changes that effect the error of speed estimation will effect the estimation of distance as well. From Figure 4.4 the following are observed,

- The highest MAPE values are observed at {D,5}. Corresponding,
  - *Initial Frequency = 4000 Hz (High)*
  - *Overlap Percentage = 90% (High)*
  - *Window Length = 8976 (High)*
  - SNR : All values present except from the lowest.
  - *Speed = 16.67 m/s (Low)*
  - *Bandwidth = 200 Hz (Low)*

* In the section 4.3.1, low speed and low bandwidth are found to effect the estimation of speed substantially. Since they are observed to be low at these coordinates, they may have a contribution to the error of distance estimation.

* The window length is high which decreases the time resolution and contributes to the error of distance estimation.

* The overlap of windows are high which would increase the time resolution, however, due to high error is observed, the effects of low speed and low bandwidth are seemed to be more dominant.

- Another high valued small group of MAPE values are observed at {A,2}. Corresponding,
  - *Initial Frequency = 200 Hz (Low)*
  - *Overlap Percentage = 50% (Low)*
  - *Window Length = 1000, 2000 (Low, Moderely Low)*
  - SNR : All values present except from the lowest.

  - *Speed = 16.67 m/s (Low)*
  - *Bandwidth = 200 Hz (Low)*

* The low frequency, low speed and low bandwidth values makes it harder to accurately detect the slope. They are also found to be the parameters that effect the speed estimation negatively when low. From the increase of the speed estimation error, the distance estimation is effected.

* Along with the low window length, low window overlap is another parameter that effected the distance estimation by effecting the accuracy of t_a estimation.

* SNR values are seemed not to have a significant effect on the observed error.

- A group of high MAPE values are observed at {B,1}. Corresponding,
  - *Initial Frequency = 200 Hz (Low)*
  - *Overlap Percentage = 75% (Moderate)*
  - *Window Length = 8976 (High)*
  - SNR : All values present.
  - *Speed = 257.22 m/s (High)*
  - *Bandwidth = 1300 Hz (High)*

* While high speed and bandwidth values contribute to a apparent slope, high window length results in a decrease in time resolution. Combined with the effect of low frequency, this decrease in the time resolution causes the observed error.

* The moderate levels of the overlap is expected to decrease the error, however, it was not high enough to negate the effect of the window length.

* The change in the SNR value is seemed to have no significant effect on the observed error.

- On the other values of the parameters, the algorithm is observed to have a moderate to high performance.

4.4 Overview of the Parameter Effects on the Performance

From the observation of self organizing maps, some parameters are found to have a common effect both on sinusoidal pulse an rectangular linear chirp due to the similarities in the algorithms.

- The effects of Doppler on the signal are less visible in the case of low initial frequency and low speed (the theoretical reasons are explained in Chapter 2). Therefore, the accuracy of speed algorithms decreases in general for these cases. The bandwidth parameter m, has also a similar effect to that of initial frequency for the linear chirp case.
- The window length determines the resolution of the spectrogram. As it increases, the frequency resolution increase. Since the algorithm uses the spectrogram's frequency values, its accuracy increases with an increasing window length.
- On the other hand, the time resolution decreases with increasing window length. This would effect the estimation of arrival time. Then the distance estimation would be effected from this decrease.
- The effects of high window length on the time of arrival estimation can be decreased by increasing the overlap of the windows, since it would increase the time resolution.
- SNR value, for all the algorithms, seemed to have almost no significant effect on the performance. The lowest SNR value tried was -2dB and with lower SNR values, its effect on the performance would be more clear. However, our algorithms seemed robust to compensate the effects of the selected SNR values.

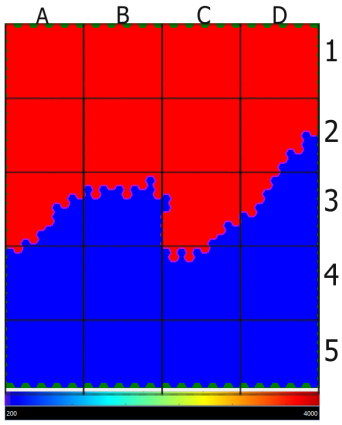

(a) Frequency Values of the Signal.

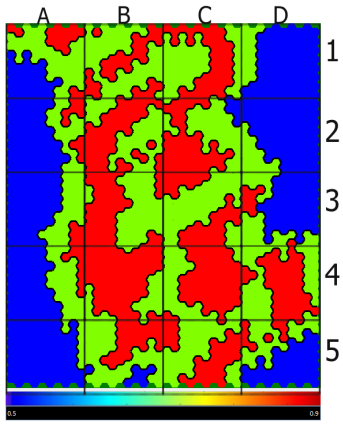

(b) Overlap Values for the STFT.

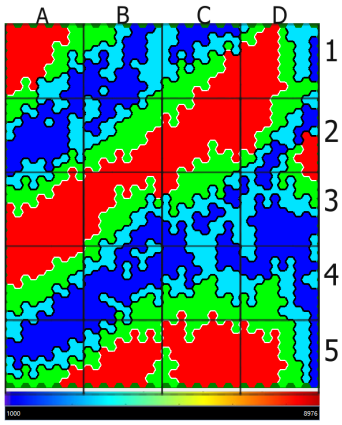

(c) Window Length Values for the STFT.

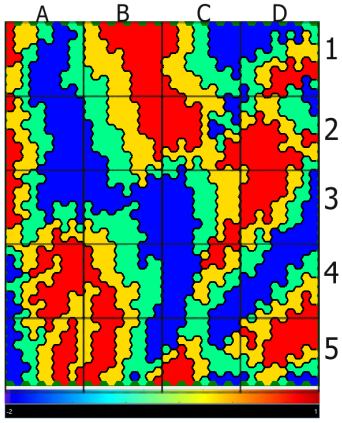

(d) SNR Values for the Additive Gaussian White Noise.

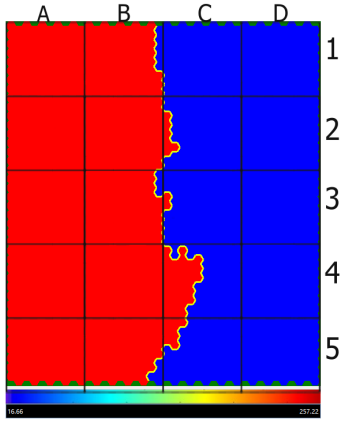

(e) The Speed of the Vehicle.

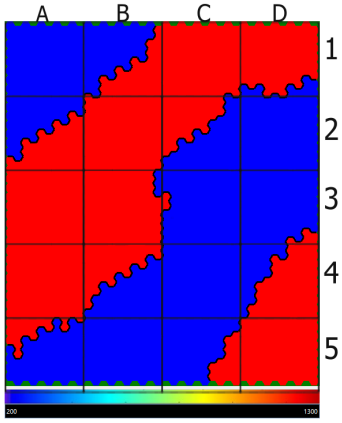

(f) Values of Bandwidth Parameter m.

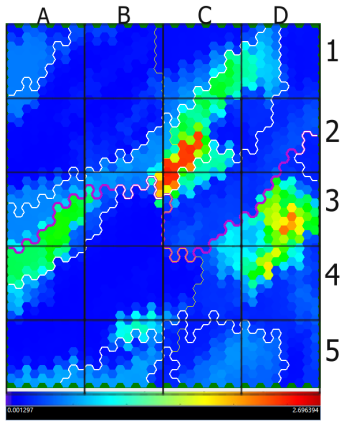

(g) Error Distribution.

Figure 4.3: Self Organizing Maps of the Parameters for Speed Estimation with the Rectangular Windowed Linear Chirp.

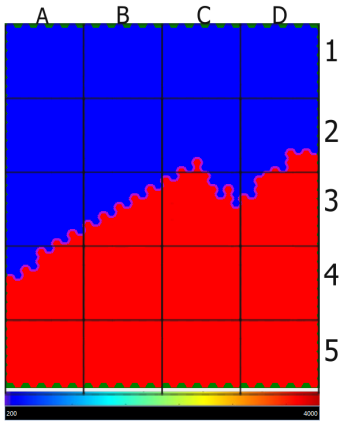

(a) Frequency Values of the Signal.

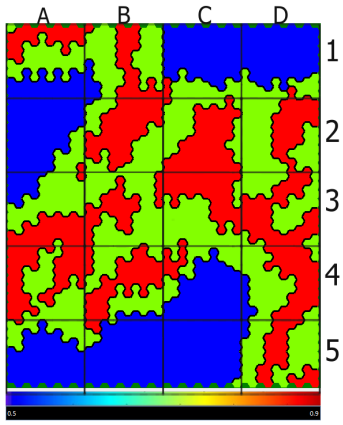

(b) Overlap Values for the STFT.

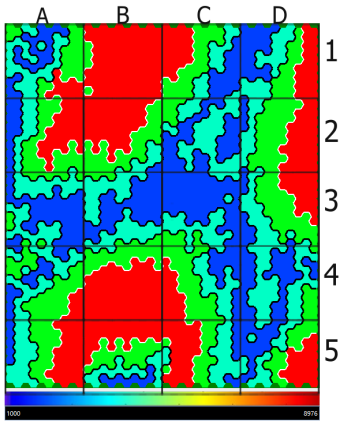

(c) Window Length Values for the STFT.

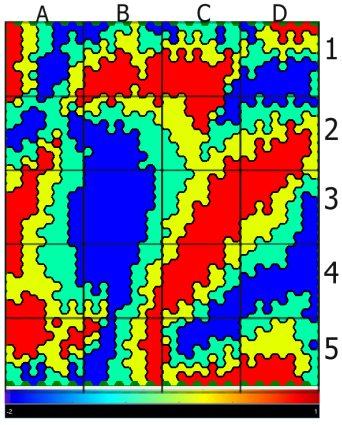

(d) SNR Values for the Additive Gaussian White Noise.

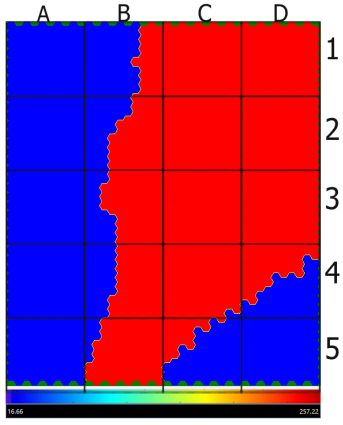

(e) The Speed of the Vehicle.

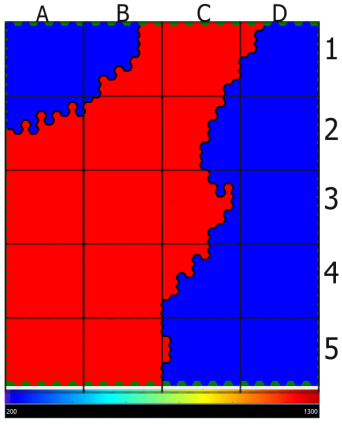

(f) Values of Bandwidth Parameter m.

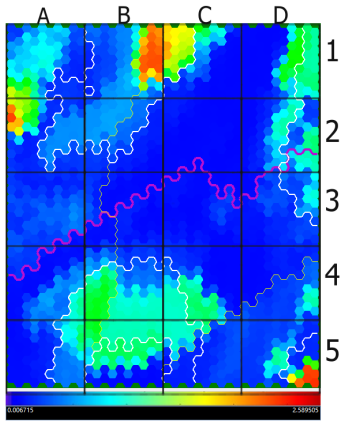

(g) Error Distribution.

Figure 4.4: Self Organizing Maps of the Parameters for Distance Estimation with the Rectangular Windowed Linear Chirp.

Chapter 5

Conclusion

In this project, a Doppler effect based velocity and distance estimation algorithm is implemented for a vehicle with constant speed emitting either a sinusoidal pulse or a rectangular windowed linear chirp sound signals. The observed signals were wrapped and delayed signals with additive Gaussian white noise. Due to the randomness of the noise, the system was tested with 30 Monte Carlo trials for each parameter configuration (192 parameter configurations for sinusoidal pulse, 384 parameter configurations for linear chirp). The MAPE and STDs of Monte Carlo trials are logged for each cell of parameter grids. The trends of error with respect to parameter distributions are observed with self organising maps and effects of parameters on estimation performance are discussed.

As a conclusive summary of the effects of parameters on performance, general MAPE and Error STD tables in Appendix A are prepared. All the mentioned trends can be observed with their corresponding average performance measures. As a final performance measure of implemented algorithms on conducted tests, overall MAPE and STD of error are found.

As it can be seen from the Table 5.1 the overall MAPE of estimations from sinusoidal signals is quite low,$\sim$ 4%. Meanwhile the estimations with chirp have a MAPE of $\sim$ 26% . However when the median of error is calculated for the estimations from chirp, it was seen that the estimation performances of two algorithms were quite close ($\sim$ 4% and $\sim$ 9% for sinusoidal pulse and chirp respectively).This was expected

Table 5.1: Table of algorithm performance figures.

	Sinusoid			Chirp	
	MAPE	STD	MEDIAN	MAPE	MEDIAN
Speed	0.04247	0.051503	0.008447	0.268904	0.095462
Distance	0.095827	0.02093	0.024837	0.351314	0.124682

since both algorithms share the same underlying principles on estimations. Hence we have concluded that the high overall MAPE from chirp estimations is due to significantly high error at certain parameter values. Therefore overall MAPE of estimation from chirp algorithm do not reflect the actual trend of performance. This can also be seen from the self organising maps for chirp signal where the overall error is observed to be distributed on quite low values.

The conducted tests are included as Excel sheets (TESTRESULTSCHIRP.xlsx and TESTRESULTSINUS.xlsx) in the submission folder and omitted from appendix due to their sizes.

As the outcomes of this project, Doppler effects are studied, hands-on experience on Doppler based estimation of distance and speed is gained, Monte Carlo simulation is learned and applied on the implemented systems. Multi-dimensional data presentation methods are searched and Self Organizing Maps are experimented with. All things considered, the project was constructive and enjoyable in terms of applications of discrete time signal processing.

Appendices

Appendix A

Table of Estimate MAPEs and STDs for Sinusoidal and Linear Chirp Signals

Table A.1: ESTIMATE MAPEs AND STDs FOR SINUSOIDAL SIGNALS

	Values	Speed Est. MAPE	Speed Est. STD	Distance Est. MAPE	Distance Est. STD
SNR	-2	0.069624438	0.142469184	0.103756622	0.063050454
	-1	0.040084022	0.027977189	0.092232473	0.007413043
	0	0.033782371	0.023364062	0.09406146	0.008922116
	1	0.026388711	0.012203064	0.093256393	0.004335396
Overlap	0.5	0.033234096	0.036273179	0.094789416	0.004847332
	0.75	0.047726797	0.082217342	0.08989423	0.040108788
	0.9	0.046448764	0.036019604	0.102796564	0.017834637
Window	1000	0.103949529	0.193009695	0.25458172	0.058355239
Length	2000	0.029916415	0.007696716	0.041649964	0.018801107
	5000	0.01330751	0.001530978	0.037847865	0.0016187
	8976	0.022706087	0.003776111	0.0492274	0.004945962
Speed	16.66	0.078585542	0.100694598	0.163653275	0.036934043
	257.22	0.005478561	0.001250226	0.02602439	0.00449491
Initial	200	0.069550267	0.046012693	0.161224248	0.016814
Frequency	4000	0.015389504	0.056994057	0.030429226	0.025046504

Table A.2: ESTIMATE MAPEs FOR SINUSOIDAL LINEAR CHIRP

	values	Speed Est. MAPE	Distance Est. MAPE
SNR	-2	0.281869297	0.357737481
	-1	0.26439806	0.350047806
	0	0.246662362	0.338059298
	1	0.236449406	0.331608205
Overlap	0.5	0.271594096	0.354431973
	0.75	0.265091004	0.349190212
	0.9	0.261604672	0.346611295
Window	1000	0.269069715	0.352358969
Length	2000	0.265109799	0.34843929
	5000	0.263010374	0.346290638
	8976	0.263818028	0.346817571
Speed	16.66	0.286616467	0.360103651
	257.22	0.226336999	0.323383578
Initial	200	0.286297494	0.373620148
Frequency	4000	0.233954955	0.317414468
Bandwith	200	0.31611417	0.394369118
	1300	0.22169466	0.308258923

References

[1] S. Barnwal, R. Barnwal, R. Hegde, R. Singh, and B. Raj, "Doppler based speed estimation of vehicles using passive sensor," in *2013 IEEE International Conference on Multimedia and Expo Workshops (ICMEW)*, 2013, pp. 1–4.

[2] Y. Liu, Y. Jia, X. Zhang, Z. Liu, Y. Ren, and B. Yang, "Noise test and analysis of automobile engine," *Applied Mechanics and Materials*, vol. 307, pp. 196–199, 02 2013.

[3] S. Khardi, "An experimental analysis of frequency emission and noise diagnosis of commercial aircraft on approach," vol. 26, 2008, p. 290.

[4] W. W. LaMorte, "Central limit theorem," July 24, 2016.[Online]. Available: https://sphweb.bumc.bu.edu/otlt/MPH-Modules/BS/BS704_Probability/BS704_Probability12.html#:~:text=The%20central%20limit%20theorem%20states,will%20be%20approximately%20normally%20distributed. [Accessed: Jan. 31, 2021].

[5] J. O. Smith, *Spectral Audio Signal Processing*. `http:`http://ccrma.stanford.edu/ jos/sasp/`//-ccrma.stanford.edu/~jos/sasp/`, [Accessed: Jan. 31, 2021], online book, 2011 edition.

[6] E. L. Oral and M. Oral, "Predicting construction crew productivity by using self organizing maps," *Automation in Construction*, vol. 19, no. 6, pp. 791 – 797, 2010. [Online]. Available: http://www.sciencedirect.com/science/article/pii/S092658051000066X